Strathprints Institutional Repository

Hantal, Gyoergy and Sega, Marcello and Kantorovich, Sofia S and Schröder, Christian and Jorge, Miguel (2015) The intrinsic structure of the interface of partially miscible fluids : an application to ionic liquids. Journal of Physical Chemistry C. ISSN 1932-7447 , http://dx.doi.org/10.1021/acs.jpcc.5b09810

The Intrinsic Structure of the Interface of Partially Miscible Fluids: an Application to Ionic Liquids

György Hantal,[*,†,‡] Marcello Sega,[†] Sofia Kantorovich,[†] Christian Schröder,[¶] and Miguel Jorge[§]

[†] *University of Vienna, Department of Computational Physics, Sensengasse 8/9, 1090 Vienna, Austria*

[‡] *Department of Chemistry, Eszterházy Károly College, Eger, Hungary*

[¶] *University of Vienna, Department of Computational Biological Chemistry, Währingerstrasse 17, 1090 Vienna, Austria*

[§] *Department of Chemical Engineering, University of Strathclyde, Glasgow, United Kingdom*

E-mail: gyorgy.hantal@gmail.com

Abstract

We investigate by means of Molecular Dynamics simulations how the intrinsic surface structure of liquid/liquid interfaces involving ionic liquids depends on the opposite phase of varying polarity. We study 1-n-butyl-3-methylimidazolium hexafluorophosphate (BMIM PF_6) and 1-n-butyl-3-methylimidazolium bis(trifluoromethylsulfonyl)imid (BMIM NTf_2). The opposite phase is either cyclohexane or water, but as a reference, IL – vacuum interfaces are also studied. We combine a distance-based cluster search algorithm with the ITIM intrinsic analyzing method to separate liquid phases showing non-negligible mutual miscibility and to identify atoms residing at the instantaneous surface. In contrast to the well structured surface of IL – vacuum systems, at liquid/liquid interfaces of ILs density correlations, ionic associations and orientational preferences are all weakened, this effect being much more pronounced when the other species is water. In such systems we observe a drastic reduction in the presence of the cation at the surface and an increase of appearance of polar moieties (of both the cations and anions) leading to decreased apolar character of the interface. Furthermore, cations are mostly found to turn with their butyl chains toward the bulk while having their methyl groups sticking towards water. Anion-cation associations are reduced and partially replaced by water-anion and rarely also water-cation associations.

Introduction

Ionic liquids (ILs) have been the subject of vast research activity in the past two decades. Indeed, ILs were found to outperform many traditional organic solvents in a wide variety of industrial processes while at the same time, their application seems to constitute minor hazard for the environment.[1,2] ILs are low temperature molten salts consisting entirely of bulky organic cations and inorganic or organic anions. Besides their inherent ionic character, these bulky ions also have an increased non-ionic nature manifesting itself through high polarizability, rather diffuse electronic density, and the separation, within the same ions, of rather ionic (polar) moieties from non-ionic (apolar) ones. The greatest potential in the application of ILs emerges from the tunability of their physico-chemical properties through accurate chemical functionalization.

A large number of studies have been dedicated so far to assess structure and dynamics in bulk ionic liquids.[3] However, many technologically important applications rely on properties of ionic liquids at interfaces with other solvents – examples being liquid extraction, or heterogeneous synthesis and catalysis.[2] Although non-negligible effort has been dedicated to experimentally assess the structure of ionic liquid interfaces,[4] our knowledge on such systems is still very limited due mostly to the reduced dimensionality of interfaces. As an alternative to experimental techniques, atomistic computer simulations have proven to be important in complementing our understanding on ionic liquid properties. In addition to the low dimensionality of interface systems, another difficulty in studying fluid interfaces occurs from the thermally induced capillary waves, which result from the coupled collective thermal motion of interface molecules: Capillary waves make the shape of the interface, as well as the identity and orientation of its constituent molecules, constantly change.[5]

Conventional analyzing techniques in computer simulations are based on a *global* view, which simply neglects the fluctuating nature of fluid interfaces and defines spatial correlations (e.g. density) with respect to a molecularly flat macroscopic surface (e.g. the Gibbs dividing surface). However, missing the *actual* location of the interface leads to faulty estimation of atomic distances from the interface and consequently to smeared structural information. Properties computed for surface molecules are also impaired in the global view by the systematic misidentification of molecules residing at the surface.

A large body of computational studies have been devoted to study liquid/vapor interfaces of neat ionic liquids as well as their mixtures. Examples can be found e.g. in Refs.[6–15] Most of the computational effort has been focused on alkylimidazolium cations in combination with halides, BF_4^-, PF_6^-, and NTf_2^- anions. All these studies found considerable layering at the interface with ions strongly aligned leading to enhanced packing. Diffusion as well as reorientational and translational dynamics were found significantly affected by the interface. In contrast, liquid/liquid interfaces involving ionic liquids, to the best of our knowledge, have been studied with molecular simulations only in a few cases: Lynden-Bell and coworkers studied interfaces between an ionic liquid and two kinds of Lennard-Jones fluids,[16] while Chaumont et al. as well as Iwahashi et al. and later Konieczny and Szefczyk studied IL – water interfaces.[17–19] Recently Iwahashi and coworkers performed simulations of a IL – butanol liquid/liquid interface.[20] All liquid/liquid and almost all liquid/vapor interface studies used the global approach, hence suffered from an inherent interpretation ambiguity bound to the misidentification of surface molecules.

The past 15-20 years have seen the development of advanced *intrinsic* experimental (e.g. sum frequency generation spectroscopy) and numerical techniques that have the necessary temporal and spatial resolution characteristic of interface fluctuations and are thus able to probe locally the instantaneous interface. The first, approximate, numerical technique developed in this spirit was proposed by Linse[21] and Benjamin[22] already two decades ago. Later, more sophisticated methods were also developed such as those by Chacón and Tarazona,[23] Chowdhary and Ladanyi,[24] Jorge and Cordeiro,[25] and Pártay et al.[26] As was shown by Jorge et al., by fine tuning an appropriately chosen control parameter all above methods can yield a consistent set of surface atoms.[27,28] Among all of them, the method by Pártay et al. (presented in detail in Section 'Materials and methods') has proven particularly versatile, useful and computationally efficient, as has been demonstrated by a long list of studies on a large variety of liquid/vapor as well as liquid/liquid interfaces of single and multi-component fluid systems.[26,29–36]

In two previous papers we presented the first intrinsic studies on the structure of the liquid/vapor interface of alkylimidazolium-based ionic liquids. In particular, we investigated how the surface structure varies by systematically changing the alkyl chain length (ethyl, butyl, hexyl), the anion (Cl^-, BF_4^-, PF_6^-), the temperature (300-360 K), and the molecular model (united-atom vs all-atom models).[6,7] Among others, we assessed how the prevalence of the most typical cation orientations change when changing the above molecular characteristics (the orientation of the studied anions was irrelevant due to their high symmetry). We found the intrinsic analysis indispensable to correctly analyze the preferred orientations of cations as it allowed us to observe an orientation that had not been identified before: this orientation (termed as "orientation III") implies the cation ring is perpendicular to the interface with the alkyl chain pointing inward, toward the bulk. Later Lísal and co-workers also used intrinsic analysis to study the structure and dynamics of the liquid/vapor interface of neat alkylmethylimidazolium (butyl, hexyl, octyl) NTf_2 as well as of butylmethylimidazolium NTf_2 with an adsorbed n-hexane layer of varying thickness on top of it.[8,9]

In this paper we report the first intrinsic study of liquid/liquid interfaces involving ionic liquids. More importantly, this essay is also one of the few computational studies on interfaces of partially miscible liquids. Despite their high importance, such liquid/liquid interfaces have received little attention. Biphasic systems of partially miscible liquids need typically long simulation times (on the order of tens or hundreds of ns) to ensure solvation equilibrium is established and the sampling of equilibrium configurations is performed efficiently. These studies have become recently possible thanks to the availability of highly parallel GPU-aided molecular dynamics softwares.[37] For our study we chose two popular members of the undoubtedly most studied imidazolium family: 1-n-butyl-3-methylimidazolium (BMIM) hexafluorophosphate (PF_6) and 1-n-butyl-3-methylimidazolium bis(trifluoromethylsulfonyl)imid (NTf_2). While the former is known to show slight instability in water as it slowly undergoes hydrolysis,[38] the NTf_2^- anion is totally water-stable hence recently favored over PF_6^-. Both of these compounds are described as hygroscopic (i.e. they absorb humidity from air) but at the same time also hydrophobic due to the relatively big apolar butyl chain of the cation and the low basicity of the anions. Indeed, the excess electronic charge on these ions is highly delocalized on many atoms leading to diffuse charge density and consequently rather low ionic character. In order to have a comparison of the effect of an apolar as well as a polar solvent on the surface structure of ILs, we chose to study ILs in combination with either cyclohexane or water. As a matter of fact, IL – water mixtures as well as interface systems are of tremendous technological importance and have thus garnered considerable attention.[39–44] Figure 1 summarizes the studied liquid/liquid interfaces. As a reference, we also present results obtained on the liquid/vapor interface (technically liquid-vacuum interface due to the low vapor pressure of ILs) of both ionic liquids.

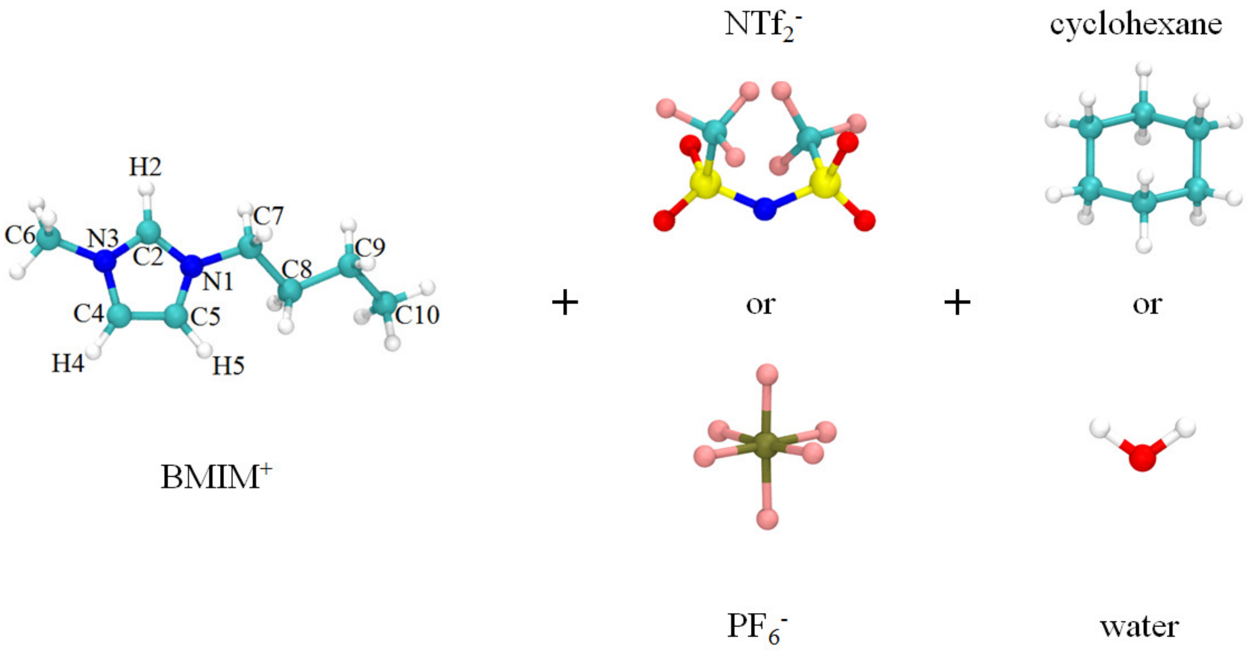

Figure 1: Components constituting the studied liquid – liquid interface systems. These systems are: BMIM NTf$_2$ – cyclohexane, BMIM NTf$_2$ – water, BMIM PF$_6$ – cyclohexane, and BMIM PF$_6$ – water. As a reference, the liquid/vapor interface of both IL species was also simulated. In this figure the atomic labels of the cation are also displayed. Hydrogen, carbon, oxygen, phosphorus, sulfur, nitrogen, and fluor atoms are represented with white, turquoise, red, brown, yellow, blue, and pink spheres, respectively.

Theoretical Methods

Computational Details

Molecular dynamics simulations were carried out with the GROMACS 4.6.7 simulation program package.[37,45] Liquid/liquid interface systems were simulated on the isobaric-isothermal ensemble at ambient conditions (298.15 K and 1 bar) by keeping the cross-sectional area of the simulation box fixed to 5.7 x 5.7 nm^2 and letting only the box length perpendicular to the interface (z direction) vary. Liquid/vapor interfaces were also simulated as a reference in the canonical ensemble at constant temperature (298.15 K) and volume with box lengths in the x and y directions equal to 5.7 nm, whereas the z length was set to high enough values ensuring that the two liquid/vapor interfaces created in the box are at least 12 nm far from each other. To keep the temperature constant in all simulations we used the Nosé-Hoover thermostat,[46,47] while constant pressure was maintained with the Parrinello-Rahman barostat.[48] To ensure fast equilibration and an efficient sampling we kept all bond lengths fixed, but the remaining degrees of freedom were free to move. This made it possible to safely use a time step for the numerical integration of the equations of motion as large as 2 fs. All non-bonded interactions were truncated beyond the spherical cut-off of 1.2 nm. To account for the long range part of the electrostatic interactions we applied the PME implementation of the Ewald summation scheme.[49] Corrections of the truncated dispersion interaction were used when calculating energy and pressure. We applied periodic boundary conditions in all directions, which, due to the particular geometry of the simulated system, led effectively to simulating a stack of liquid slabs. The electrostatic energy of periodic systems includes a shape-dependent term, which, for the slab case, depends on the average dipole moment of the simulation box,[50] and can in principle be accounted for by using different correction schemes.[51,52] In the present case, however, since the average dipole moment of the system is zero, the correction is not necessary.[51]

In the first step each neat liquid phase was separately equilibrated as bulk in the NpT ensemble. For IL phases, simulations were started from previously equilibrated configurations of 512 ion pairs. For the other liquids, initial configurations were created by randomly placing 7500 water or 1000 cyclohexane molecules in a box by avoiding overlaps. To create liquid/vapor interfaces we extended the box of the previously equilibrated bulk liquids in the z direction (and obtained two liquid/vapor interfaces). In the case of liquid/liquid interfaces, the two neat liquids were placed next to each other leaving some free space in between to avoid overlaps, after which we performed a short simulation (500 ps) in the NpT ensemble for the system to be able to close this gap and reach a near equilibrium volume. From the resulting configuration further equilibration was launched aiming at reaching a system of two liquids of equilibrium composition. The latter was monitored through the size of the largest clusters of each species (see below). Due to the high viscosity of some systems, in certain cases equilibration lasted as long as a few hundred ns. In the next step, production runs were performed to sample equilibrium configurations. This lasted for 100 ns for liquid/liquid interfaces yielding a sample of 10000 configurations, and 20 ns for liquid/vapor interfaces to obtain a sample of 4000 configurations.

Molecular models

Choosing a reliable atomistic model for ionic liquids that gives accurate description of most properties is a non-trivial task. Indeed, early ionic liquid force fields aimed for generality and simplicity therefore net charges on ions were set to their integer nominal value. However, it turned out that while these force fields are able to reproduce static properties with a certain accuracy, their performance is poor in terms of dynamics: the predicted viscosities are way too high and the computed diffusion coefficients are too low compared to the actual experimental values. Later on, many studies have suggested that using integer charges leads to a system much too cohesive probably due to the exaggerated ionic character that fixed point charge models (lacking sufficient level of sophistication) can provide.[53–56] In reality, the bulky ions of ionic liquids have more molecular character due to their high polarizability and the high degree of delocalization of their charge density. It has also been shown that the reduced ionic character can be accounted for in an effective way by setting ionic net charges, in absolute terms, to less than unity leading to the emergence of a series of new ”reduced charge models”.[17,53–56] Note that these models treat the effect of polarization in a simplified manner by fixed reduced ionic charges which makes the model unable to adapt to local changes of the electric field. As the degree of polarization varies significantly from one ionic liquid to another these modified force fields are designed to accurately describe one single ionic liquid species, thus precluding general transferability. In a notable study, Köddermann and coworkers showed that the correct reproduction of both static and dynamic properties is possible also by leaving overall charges on anions and cations set to unity but reducing the LJ parameters of certain atoms (i.e. weakening dispersion interactions).[19,57] This result confirms that the main issue with the original integer charge models is that they are too cohesive (i.e. the internal energy is too low). However, in spite of the success of this effective model in reproducing physico-chemical properties, the physicality of leaving the provenly exaggerated ionic character unchanged is debatable.

As the accurate description of molecular interactions between ILs and other liquids is key to reproducing the right solubility, interfacial thermodynamics (e.g. interfacial tension), and consequently the interface structure, we chose to use computationally efficient reduced charge models to describe ionic liquid interactions. The importance of choosing such models became obvious when, as a first trial, we set up the BMIM PF_6 − water interface using the Canongia-Lopes–Pádua force field[58] in combination with the TIP4P water model[59] and we obtained a totally miscible system as opposed to experimental observations. This is in accordance with the findings of Chaumont et al. who scaled overall charges on BMIM PF_6 to ±0.9e to obtain more realistic solvation properties with water.[17] To describe the BMIM PF_6 ionic liquid we chose the force field developed by Bhargava and Balasubramanian which sets the total charge on ions equal to ±0.8e.[53] We found this model to describe density as well as dynamic properties with a good accuracy. To model BMIM NTf_2 we applied the force field published by Logotheti et al. that sets net ionic charges to ±0.9e and which the authors reported to reproduce experimental densities as well as self-diffusion coefficients at acceptable precision.[60] Both force fields are fully flexible and contain bond stretching, angle bending as well as proper and improper torsional potentials. A series of the most typical solvents were chosen as opposite phase to study their liquid/liquid interface with the two ionic liquids: Acetonitrile, dimethyl sulfoxide, hexanol, benzene, cyclohexane, and water. However, the first two solvents proved to be totally miscible with both ionic liquids. The IL-hexanol systems turned out to be very viscous making the equilibration extremely long (more than 0.5 μs) at ambient conditions. In turn, while the solubility of both ionic liquids was basically negligible in benzene, the solubility of benzene in ILs turned out to be so high (in accordance with experimental observations)[61] that the separation of the two phases was not feasible by means of the simple cluster counting algorithm since benzene molecules formed a fully percolating network in the whole system. For this reason, we also omit these systems from the current study. We were eventually left with cyclohexane and water. For all organic solvents we applied the OPLS force field, while for water we compared four popular models (SPC, SPC/E, TIP4P, and TIP4P2005) and chose eventually SPC[62] as it showed the best overall performance regarding solubility and interfacial tension estimates with both ionic liquids. Although not discussed here in the paper, we included snapshots of IL – hexanol and IL – benzene systems in SI. Also, interfacial tension and solubility values are presented in SI as calculated for IL – water systems, computed with the four popular water models.

Separation of phases of partially miscible liquids

The primary purpose of the ITIM analysis is to identify atoms residing at the surface of fluid phases. If the ITIM analysis is to be performed on a liquid/liquid interface first one has to unambiguously separate molecules belonging to one or the other phase. No complication arises if the two species do not mix and hence each species constitutes one single phase. In such a case, the terms “species” and “phase” can be used almost interchangeably. However, if the two species exhibit non-negligible miscibility the phases are not neat and the separation of molecules making up the different phases is needed. This, in general, is a non-trivial task. In order to avoid confusion, in what follows, we will try to make a clear distinction between phases and species, and when we refer to a phase of a given species we will mean the phase rich in that particular species (bearing in mind that the phase might contain molecules of the other species).

In this work, we tackle the problem of partial miscibility by performing a distance-based cluster search that provides molecular connectivity and the corresponding molecular clusters. The threshold distance beyond which two atoms are not considered belonging to the same cluster was set separately for each species based on the location of the first minimum in the corresponding radial distribution functions. In a biphasic system, we define the phase rich in a given species as the union of the largest cluster of that species and all smaller-than-largest clusters of the other species. Unfortunately, this basic cluster search based scheme can be used only when the partial miscibility of the species is relatively low: the algorithm works fine if the molecules of a given species assemble into one major cluster and a couple of well separated molecular aggregates solvated in the other phase. However, this may not be fulfilled if the minor clusters are of a size comparable to that of the largest cluster. Another problematic situation is when the molecules form fingers deeply protruding into the opposite phase. In an extreme case, the system might become fully percolating for one or both species (i.e. it becomes bicontinuous), while still forming two distinct phases where densities are markedly different. In such cases, more involved algorithms would be needed to accurately distinguish the two phases

Intrinsic surface analysis: the ITIM method

The intrinsic analysis, in the first place, yields the complete list of surface atoms by which the surface is unambiguously defined according to the capillary wave theory. To identify surface atoms we use the "Identification of Truly Interfacial Molecules" (ITIM) method.[26] This method consists in "dropping" probe spheres, organized on a grid, from the opposite phase onto the phase to be analyzed. Probe spheres are "moved" along a direction parallel to the macroscopic surface normal until they "touch" the first atom which is then labeled as surface atom. In this analysis, we represent atoms with spheres of a diameter equal to their Lennard-Jones distance parameter σ. When all probe spheres have been dropped the complete list of interface atoms is readily available. To have a continuous intrinsic surface defined at any (x,y) points we use a linear triangular interpolation scheme.[25,27] Such an algorithm was found to be a very efficient way of accurately computing intrinsic distances ($z_{intrinsic}$) and, based on them, intrinsic profiles. The result of the cluster search in combination with the ITIM analysis is illustrated in Figure 2 with an equilibrium snapshot from the BMIM NTf_2 – water system: molecules solvated in the opposite phase (drawn as large yellow and purple spheres for the IL and water, respectively) are highlighted as well as atoms constituting the IL-rich phase (large red spheres).

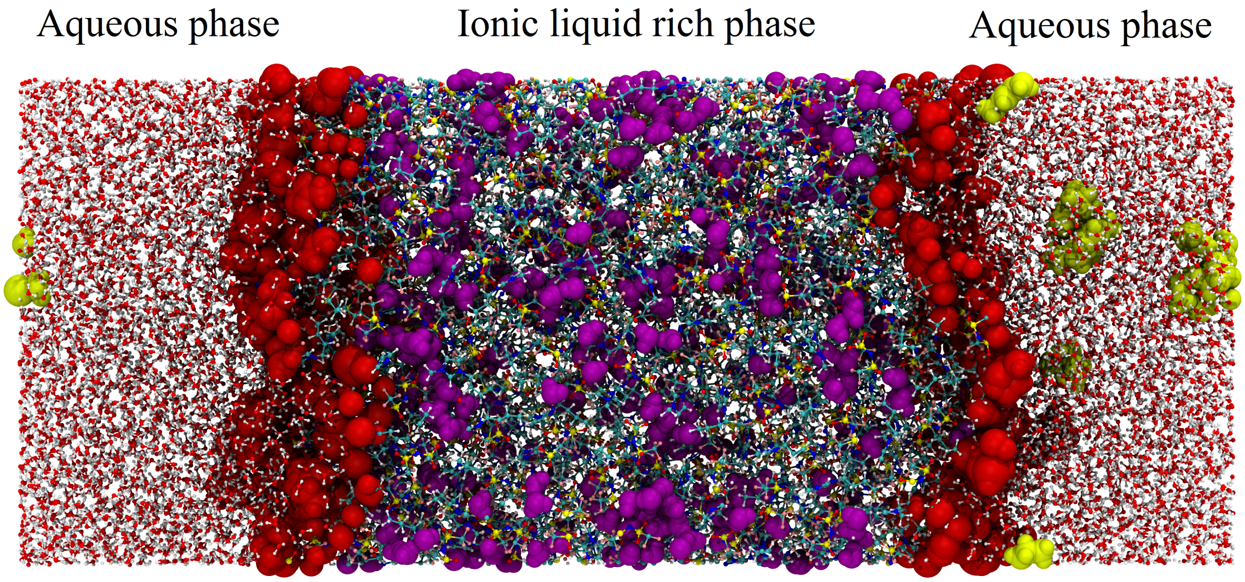

Figure 2: Result of the combination of the ITIM analysis with the cluster search in an equilibrium snapshot of the BMIM NTf_2 – water interface system. The phase rich in the IL is in the middle surrounded by the aqueous phases. Note that our systems are fully periodic in all directions. The large red spheres represent the atoms found at the surface of the IL-rich phase by means of the ITIM analysis. Atoms of water molecules solvated in the IL-rich phase as well as those of cations and anions hydrated in water are drawn with large purple and yellow spheres, respectively. Their separation from their main phases was determined by a simple distance-based cluster search analysis. For an explanation of the applied color code of atoms see the caption of Figure 1.

The ITIM method makes use of one free parameter that determines its resolution, i.e. it controls the length scale of the surface roughness one can probe. It is reasonable to think that a rugged surface needs to be probed on the length scale of the particles that give rise to its roughness. Therefore the sensible choice for the size of the probe should be comparable with the average radius of the building blocks (here atoms) in the system. To be consistent with our previous studies here we chose to use probes of a radius of 2 Å. It is worth mentioning that the ITIM method has recently been generalized to be able to deal with surfaces of arbitrarily curved shapes.[63]

Results and Discussion

Equilibrium compositions

Before presenting the interface structure, we start our discussion by reporting interfacial tensions and miscibilities in the studied biphasic systems and comparing them to respective experimental values. Interfacial tension values were calculated from the virial route by integrating, along z, the difference of pressure components lateral(average of p_x and p_y) and normal (p_z) to the interface.[64] This serves, on the one hand, as validation of the chosen molecular models. On the other hand, one can benchmark the phase separating capability of the cluster analysis by comparing the obtained solubilities ($x_i^{j,clust}$) to those estimated from densities far from the inteface ($x_i^{j,dens}$):

$$x_i^{j,dens} = \frac{\frac{\rho_i^j}{M_i}}{\frac{\rho_j^j}{M_j} + \frac{\rho_i^j}{M_i}}, \tag{1}$$

$$x_i^{j,clust} = \frac{N_{tot}^i - S_{max}^i}{S_{max}^j + N_{tot}^i - S_{max}^i}, \tag{2}$$

where x_i^j is the mole fraction of species i in species j. ρ_i^j denotes the mass density of species i, calculated far from the interface in the phase rich in species j, while M_j and M_i are the corresponding molar masses. N_{tot}^i is the total number of molecules of species i in the system, while S_{max}^i denotes the number of molecules or ion pairs (i.e. the average of the number of constituting anions and cations) of species i in the largest cluster. i and $j (\neq i)$ signify any of the species in the biphasic system.

Computed and experimentally measured solubility and interfacial tension values are reported in Table 1. This table shows that, on the one hand, the BMIM NTf_2 model reproduces the experimental surface tension as well as the interfacial tension with water with an acceptable accuracy, but while the former is somewhat overestimated, the latter value is underestimated. These deviations hint that the chosen model might overestimate the polar (ionic) character of BMIM NTf_2. This conclusion is further confirmed by the fact that the mutual solubility of BMIM NTf_2 with water is roughly twice higher than the measured values. Although there are no available data regarding the miscibility of this IL with cyclohexane as well as their interfacial tension, the experimentally measured solubility of n-hexane in BMIM NTf_2 (0.095) indicates that the actual solubility of cyclohexane in BMIM NTf_2 might be higher than the computed value (0.03).[75] All things considered, we conclude that the performance of the model by Logotheti et al. is acceptable for our purposes. A possible refinement of the force field might consist in further decreasing partial charges and somewhat increasing Lennard-Jones parameters to make the model less polar.

The performance of the chosen BMIM PF_6 force field seems even better than that of the BMIM NTf_2 model. Indeed, it accurately reproduces the interfacial tension values with both cyclohexane and water, though it somewhat underestimates surface tension. What is more, the estimated solubility of this IL in water is quite close to the experimental value. The only respect where the model seems to somewhat fall short is when it comes to the solubility of water in the IL: it underperforms by 50%. As for the case of cyclohexane, we found one experimentally measured solubility value in a 2001 article by Blanchard and Brennecke,[61] but since the published value seems too high (0.21) as compared to the very low solubility of alkanes in ILs we are reluctant to use it as a reference. In the same paper total miscibility of n-hexane in BMIM PF_6 is reported, which seems incompatible with the general understanding.[65] Based on the concerns raised above, we prefer to omit the published cyclohexane solubility in BMIM PF_6 from our discussion.

Table 1: Comparison of the computed solubility and interfacial tension values for the studied interface systems composed of an IL (BMIM NTf_2 or BMIM PF_6) and another species (water or cyclohexane). Experiments and simulations were performed at 298 K and 1 bar. Solubility data (given as mole fractions) were calculated in two ways, referred to as "dens." and "clust." (see text). For better visibility, experimental solubility data are displayed bold faced.

Anion	other species		Solubility	
			IL in other sp. / 10^{-3}	other sp. in IL
NTf_2^-	cyclohexane	dens.	0	0.029 ± 0.007
		clust.	0	0.029 ± 0.005
		exp.	-	-
	water	dens.	0.5 ± 0.1	0.61 ± 0.02
		clust.	0.5 ± 0.2	0.54 ± 0.02
		exp.	**0.31**[a]	**0.25**[a]
PF_6^-	cyclohexane	dens.	0	0.006 ± 0.001
		clust.	0	0.006 ± 0.002
		exp.	-	-
	water	dens.	1.26 ± 0.07	0.14 ± 0.01
		clust.	1.0 ± 0.3	0.11 ± 0.02
		exp.	**1.28**[b]	**0.26**[c]

Anion	other species	Interfacial tension ($mN\ m^{-1}$)	
		Simulation	Experiment
NTf_2^-	vacuum	38 ± 3	32.9[d] – 38.4[e]
	cyclohexane	9 ± 2	-
	water	8 ± 2	13.2[f]
PF_6^-	vacuum	40 ± 4	43.8[g] – 48[h]
	cyclohexane	14 ± 1	13.15[i]
	water	10 ± 1	10.06[i]

[a]Ref[66] [b]Ref[67] [c]Ref[68] [d]Ref[69] [e]Ref[70] [f]Ref[71]
[g]Ref[72] [h]Ref[73] [i]Ref[74]

As long as miscibilities are relatively low, values estimated from the cluster analysis match perfectly those calculated based on bulk densities. The latter can be considered the reference method as it is defined only with bulk equilibrium properties. However, as solubilities increase, the cluster analysis systematically underestimates as is seen in the case of the solubility of water in either IL. We relate this to the ambiguity in separating molecules (e.g. those constituting fingers) belonging to one phase or the other. This shows that the macroscopic concept of the interface loses its meaning at the microscale between liquids of considerable mutual miscibility. We note that the miscibility threshold above which the cluster analysis systematically underestimates equilibrium compositions when benchmarked with values computed from bulk densities necessarily depends on the shape of the constituting ions and molecules as well as the particular topology of the given interface.

Density profiles

In Figure 3 we present profiles computed with respect to the flat macroscopic plane of the surface (i.e. global profiles, Figure 3 a-c) and those calculated with respect to the actual instantaneous surface of a phase as determined by means of the ITIM method (i.e. intrinsic profiles, Figure 3 d-f). The conventional global density profiles in Figure 3 a-c show a smooth increase near the interfacial region, while they display a wavy shape of decreasing amplitude towards the bulk. It is immediately apparent that global profiles get strongly dampened (i.e. planar layering is strongly reduced) as soon as there is another liquid phase present in the system regardless of its polarity. Moreover, the density enhancements at the liquid-vapor interfaces, plotted as black curves in Figure 3 a-c are removed at liquid/liquid interfaces. In the case of IL – water systems, the bulk ionic liquid density is lower than in the neat system due to the significant solubility of water in the IL-rich phases.

Intrinsic density profiles computed with respect to the surface of either the IL-rich or the water-rich phases displayed in Figure 3 d-f also show some noticeable features (profiles computed with respect to the surface of the cyclohexane-rich phases are not discussed due

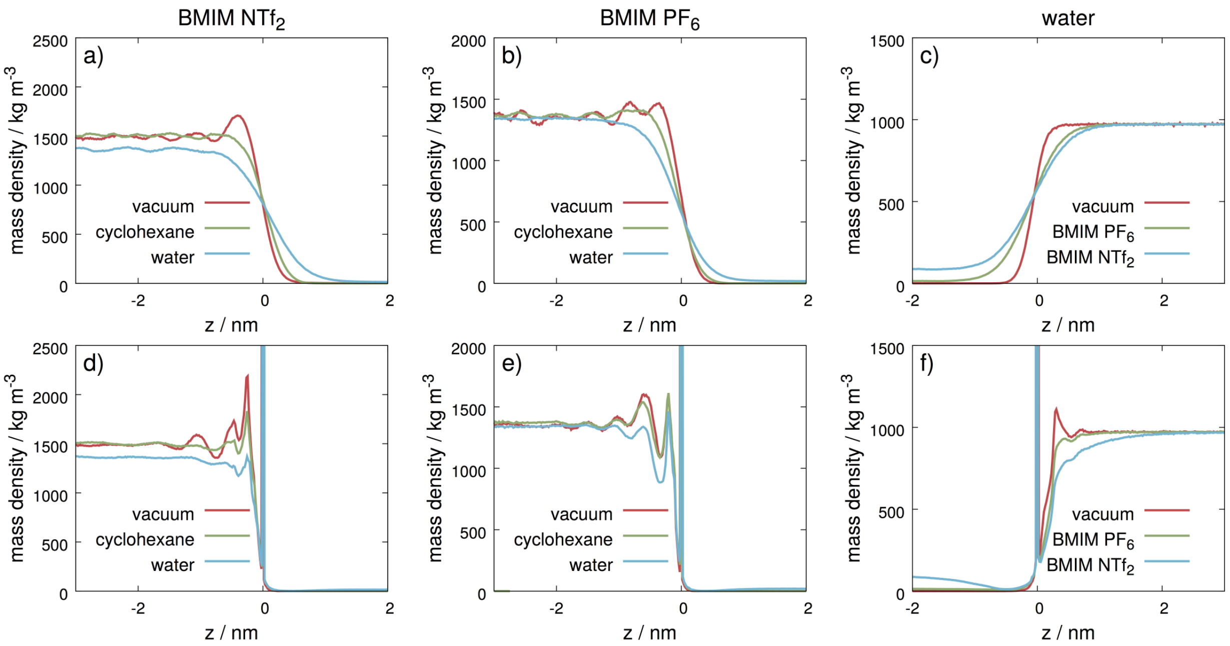

Figure 3: Comparison of global (a-c) and intrinsic (d-f) density profiles computed at all interfaces of BMIM NTf_2 (a,d), BMIM PF_6 (b,e), and water (c,f). The intrinsic density profiles were computed with respect to the surface of the phases rich in either BMIM NTf_2 (d) or BMIM PF_6 (e) or water (f). Flattening of IL density profiles can be observed as the phase opposite to the IL changes from vacuum through cyclohexane to water.

to their insensitivity to the opposite phase.) The first observation is that these intrinsic profiles display a more pronounced structure than global profiles. Right at the interface a delta-like trivial peak occurs. This is because the surface is defined by the positions of surface atoms which consequently are all at $z_{intrinsic} = 0$. As one decreases the bin width to obtain finer resolution this peak can increase to an arbitrary level. Under this layer of surface atoms there appears an immediate depleted region due to the excluded volume of surface particles, which is followed by alternating regions characterized with densities above or below the bulk value indicating positive or negative density correlations with respect to the instantaneous surface. In the case of BMIM NTf_2, the dampening of the correlations due to the other phase is more pronounced than in the systems containing BMIM PF_6: Indeed, the intrinsic density profiles of BMIM NTf_2 are almost totally flat at 0.7 - 1 nm beneath the surface. On the contrary, in systems containing BMIM PF_6 only the near interface region seems to be affected (here peak heights get lowered) while the dampening is much weaker than in BMIM NTf_2 systems. Therefore, density profiles calculated at BMIM PF_6 surfaces still show noticeable structure as deep as 2 nm under the surface, irrespective of the nature of the other fluid. The actual shape of the intrinsic density profiles is the consequence of the layering, but it is also very strongly related to the particular structure and shape of the molecules constituting the phase. This dependence, which is totally not straightforward, could be elucidated by a more thorough analysis, but as it is beyond the scope of the present paper, we leave it for a future study.

Intrinsic density profiles calculated at liquid/liquid interfaces display a decrease of the height of the second and subsequent peaks with respect to the corresponding liquid/vapor systems. This decrease can be sensibly explained by a transfer of molecules from the underlying layers to either the bulk or the surface. Generally, a decrease in interfacial tension leads to an increase in surface area, which makes it possible to accommodate more molecules at the surface. The decrease in interfacial tensions and the corresponding interface broadening observed in the mean-filed density profiles are consistent with the increase in the number of surface molecules.

At a liquid/liquid interface, the surface of both constituting phases can be identified and hence intrinsic density profiles can be computed with respect to the surface of either liquid phase. Figure 4 compares global as well as intrinsic density profiles calculated at the BMIM NTf_2-water interface with respect to either liquid phase. Intrinsic profiles computed with respect to the opposite phases (blue curve in Figure 4 b and red curve in Figure 4 c) contain information regarding how much the density of a given phase is correlated with the surface of the other phases. No correlation would result in totally flat profiles. The fact that these profiles calculated with respect to the surface of the opposite phase are not flat means that there is some correlation between the surface layering of the two phases, though it vanishes relatively soon, after one peak.

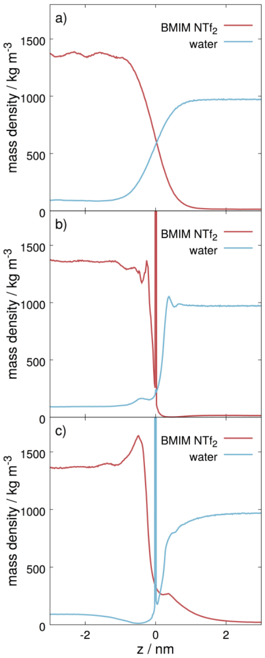

Figure 4: Global (a) and intrinsic (b and c) density profiles calculated in the BMIM NTf_2 – water system. When calculating intrinsic density profiles, the surface of the phase rich in either IL (b) or water (c) was considered as reference plane. While very little correlation is observed with respect to the macroscopic surface (a), noticeably more structured intrinsic profiles are displayed by both intrinsic curves (b and c). Note that the opposite phases also display remarkable density correlation near the interface with respect to the reference instantaneous liquid surface.

Distribution of surface atoms and molecules

In the next step we calculated the number of particles at the surface of the IL-rich phases as the opposite phase changes. Such an analysis provides information on the surface composition and the distribution of typical (groups of) atoms that the molecules of the other phase encounter at the interface. In our analysis, every ion and molecule that has at least one atom found at the surface is defined as surface ion or molecule. Note that molecules of the other species were occasionally also found at the surface. The composition of the surface layers of the IL-rich phases is given in Table 2. Composition is described with surface (number) densities which were simply calculated by dividing the average number of the given ion or molecule with the cross sectional area of box along the plane of the interface.

Table 2: The molecular surface density (see text) of anions, cations and molecules of the other species (cyclohexane or water), as well as their proportion computed at the surface of the phase rich in ionic liquid.

Anion	other species	density / nm^{-2} Anion	Cation	other	cation to anion ratio
NTf_2^-	vacuum	1.34	1.78		1.3
	cyclohexane	1.46	1.73	0.01	1.2
	water	1.89	1.91	0.06	1.0
PF_6^-	vacuum	0.99	2.17		2.2
	cyclohexane	1.31	2.13	0.01	1.6
	water	1.52	1.86	0.03	1.2

Anion	other species	Proportion Anion	Cation	other
NTf_2^-	vacuum	43.0%	57.0%	-
	cyclohexane	45.5%	54.1%	0.4%
	water	48.9%	49.6%	1.5%
PF_6^-	vacuum	31.3%	68.7%	-
	cyclohexane	38.1%	61.7%	0.2%
	water	44.5%	54.6%	0.9%

Table 2 shows a couple of interesting trends. One can immediately notice that in all cases, the total number of ions at the surface is indeed higher when the opposite phase is either liquid with respect to the liquid/vapor case. It is also readily seen that the surface is always more populated with cations than anions. This is most pronounced in the case of IL – vacuum systems. This unbalanced repartition of ions is related to the relatively small size of the anions. Indeed, the well-known high butyl chain density at the liquid/vapor interface of BMIM containing ILs leads to an efficient screening of the underlying anions such that they are not "seen" from the opposite phase. Accordingly, as the anion becomes more comparable in size with the cation (case of BMIM NTf_2) this unevenness is reduced (see Table 2). This disparity further decreases when the IL faces cyclohexane; it is even more so when the polar water is the opposite phase.

To understand better how the polarity and the coverage of the surface by different molecular moieties change from one system to the other we computed the distribution of atoms at the surface (i.e. atoms contributing to the trivial peak of the intrinsic profiles) at all ionic liquid surfaces investigated. In order to simplify discussion, we grouped H atoms with the

C atom they belong to and derived occurrences for corresponding methine (CH), methylene (CH_2) and methyl (CH_3) groups. Similarly, the occurrence of atoms of NTf_2^- anions is discussed with that of N, SO_2 and CF_3 groups. Figure 5 shows the distribution of groups at the IL-rich surfaces of BMIM NTf_2 (a-c) or BMIM PF_6 (d-f) when the opposite phase is either vacuum, cyclohexane, or water, respectively.

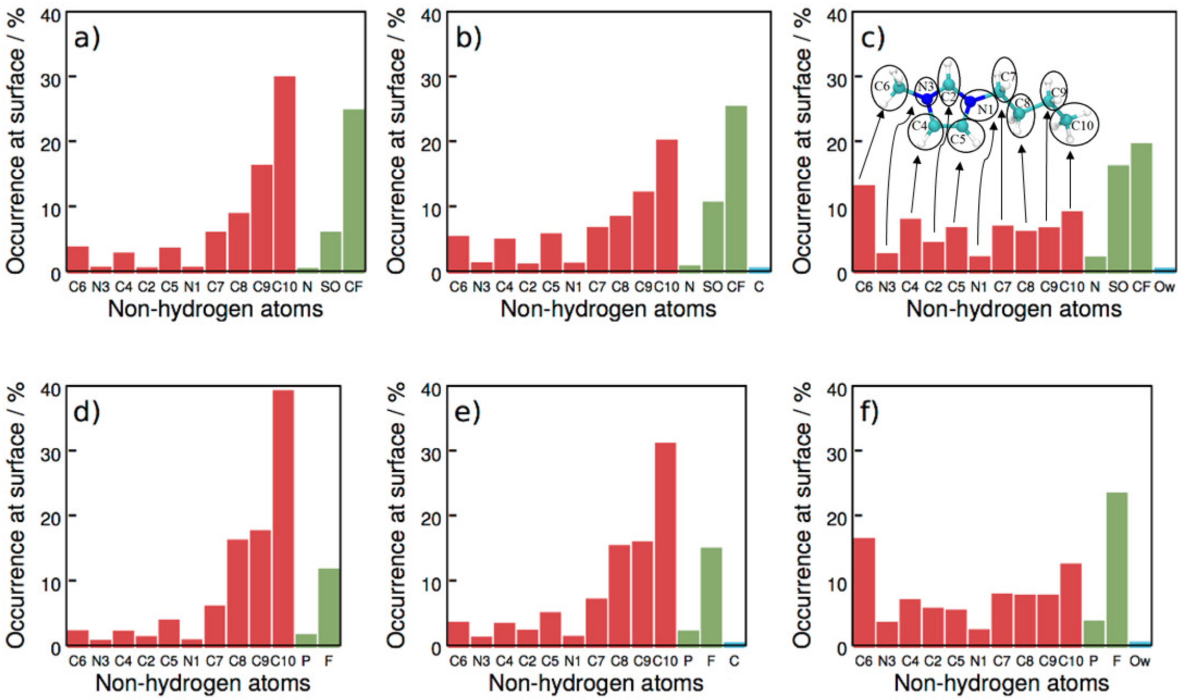

Figure 5: Frequency of identifying non-hydrogen atoms as surface atoms in the ITIM analysis at the surface of phases rich in BMIM NTf_2 (a-c) or BMIM PF_6 (d-f) while the opposite phase is either vacuum (a,d), cyclohexane (b,e), or water (c,f). As illustrated in the inset of graph c, overall counts are derived for CH_3, CH_2, and CH groups by considering the occurrence of H atoms together with that of the carbon atoms they belong to. Atoms in the NTf_2^- anions are similarly combined into groups. Red, green and blue columns correspond to groups of the cation, anion, and molecules of the other species, respectively. This analysis reveals that the occurence of butyl chains decreases while rings and anions (i.e. polar moieties) become more exposed to the surface of the IL-rich phases when the opposite phase changes from vacuum through cyclohexane to water.

Figure 5a and d reveal that in the case of the interface with vacuum, the majority of atoms at the surface belong to the butyl chain, while ring atoms are encountered only occasionally. Similarly, the apolar CF3 groups of the NTf_2^- ions are also frequently found at the surface.

This distribution noticeably changes at interfaces with cyclohexane (Figure 5b, e) where the occurrence of the last methyl (C10) and methylene (C9) groups of the butyl chain decreases, and the recurrence of ring atoms at the surface increases. This can be simply interpreted as a steric effect: Although still a considerable number of butyl chains stick out from the surface, not all of them can be incorporated in the cyclohexane phase. In the case of the interfaces with water, these tendencies become significantly more pronounced. At interfaces between both ILs and water (see Figure 5 c and f), a drastic reduction of the occurrence of butyl chain atoms is accompanied by a significant increase of the occurrence of the ring atoms. Surprisingly, the methyl ligand (C6) becomes the most frequent group of the entire cation at the surface: it appears 4 times more often at the surface than in the BMIM NTf_2 – vacuum system, while the terminal methyl group of the butyl ligand encounters a 4-fold drop in relative occurrence. At the same time, the anion's rather polar SO_2 groups become almost equally frequently found at the surface as CF_3 groups, and even the central N atom is found at the surface occasionally.

These trends show that when moving from liquid/vapor to liquid/liquid interfaces the coverage of butyl chains at the surface decreases and at the same time the polar character of the surface increases through an increase of surface density of polar moieties. This also implies that the orientational preferences of surface ions must also drastically change. This aspect is discussed in the next Section of this paper.

Orientation analysis of interface molecules

The identification of the most preferred molecular orientations at the surface provides crucial information regarding the character of the interface, which is necessary, among others, to attain a molecular-level understanding of the mechanism and kinetics of transport through the interface.

To describe the orientation of the cations we followed the same analysis applied in our previous studies on the intrinsic structure of vapor/liquid interfaces of imidazolium-based

ILs.[6,7] The orientation of both the "head" (i.e. the imidazolium ring) and the "tail" (the butyl chain) is described: in the case of the imidazolium ring which, due to its aromaticity, can be treated as a rigid body, we computed a bivariate distribution, while for the butyl chain, a univariate angular distribution. To calculate the bivariate statistics of the rings we followed the methodology proposed by Jedlovszky et al.: we compute the likelihood of observing any combinations of the angular polar coordinates ($P(\cos\theta, \phi)$) of the macroscopic surface normal ($\vec{n}$) in a coordinate frame fixed to the imidazolium ring (X',Y',Z').[76] In this frame axis Z' is chosen to point along the bisector of the vectors pointing from the C2 atom to the two N atoms, N1 and N3 (for the atomic labels see Figure 1). Axis Y' points along the N1→N3 vector while axis X' is perpendicular to Y' and Z' in a way that the (X',Y',Z') triplet satisfies the right-hand rule. Angle θ is the angle between the macroscopic surface normal ($\vec{n}$) and axis Z', while ϕ is the angle formed between axis Y' and the projection of $\vec{n}$ onto the (X',Y') plane. See Figure 6 for an illustration of the definition of these angles. The orientation of the butyl chains is described by computing the distribution of the cosine of the angle (σ) formed between the macroscopic surface normal and the vector pointing from the first nitrogen atom adjacent to the butyl chain (N1) to the last carbon atom of the butyl (C10) chain (see Figure 6).

We were also interested in describing the orientational preferences of anions. For PF_6^-, this is of no practical value due to the high symmetry of this ion, while NTf_2^- has a less symmetric, "two-armed" shape. To elucidate in what directions the "arms" point we computed the distribution of the cosine of the angle (ρ) of the vector pointing from the sulfur atom of the polar sulfonyl group to the carbon atom of the adjacent apolar CF_3 group with respect to the macroscopic surface normal (see Figure 6). In Figure 7 we display the computed orientational distributions of the imidazolium rings of BMIM NTf_2 (a-c) and BMIM PF_6 (d-f) as calculated at the interfaces between the ILs and vacuum, cyclohexane, and water.

The orientational preferences of both cations, represented as color maps in Figure 7, exhibit the very same trend, irrespective of the anion, when the opposite phase changes from

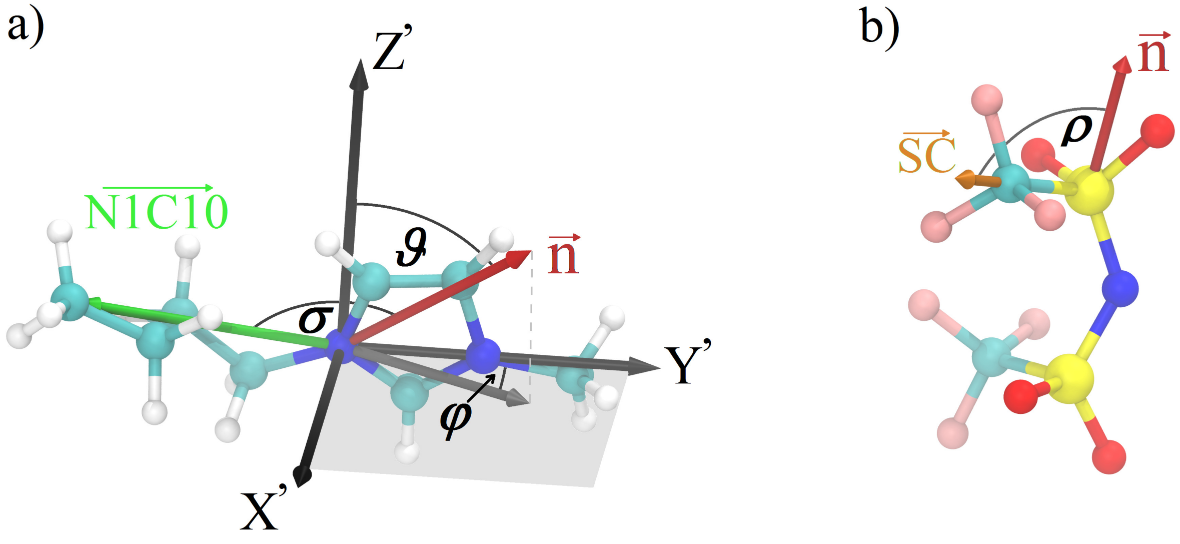

Figure 6: Definition of angles for the analysis of preferred orientations at the surface. A body-fixed coordinate frame is used to describe the orientation of the rigid imidazium rings of the cations with the polar angle coordinates θ and ϕ (a). The orientation of the butyl chains of cations (N1→C10 vector) as well as that of the apolar "arms" of the NTf_2^- anions (S→C vector) are described with the distribution of σ and ρ, respectively(a,b).

vacuum through cyclohexane to water. At the IL – vacuum interface (Figure 7 a and d) the overwhelming majority of cation rings have both a $\cos\theta$ and a ϕ value near 0. This pair of values corresponds to an orientation where the ring's plane is parallel with the surface normal and N1, to which the butyl chain is attached, points outward to the opposite phase, while N3 (on the side of the methyl substituent) points inward to the bulk. This is indeed the most typical cation ring orientation found both in experiments and simulations. In previous studies we called this orientation "orientation I".[6,7] Note that the peak for the BMIM NTf_2 – vacuum system (Figure 7 a) is shifted to slightly negative $\cos\theta$ values, which means the ring (still perpendicular to the surface) is slightly tilted in a way that its C5 atom turns towards the surface and the C2 atom turns away form it (i.e. towards the bulk). This observation is consistent with what we have found for the distribution of surface atoms. Indeed, in orientation I, due to simple geometrical reasons, C5 is expected to appear at the surface more often than the C2 atom. Such an unevenness is indeed found in the distribution of surface atoms for both cations, however it is much stronger in the BMIM NTf_2 – vacuum system (see Figure 5 a) supporting thus the slightly tilted orientation of the cations.

A secondary, weak preference appears on the map of the BMIM NTf_2 – vacuum system (Figure 7 a) at around $\cos\theta = 0$ and $\phi = 180°$. This peak corresponds to an orientation where the plane is again parallel with the surface normal but now the butyl chain is on the bulk side of the interface, while the methyl group points outward to the opposite phase. We referred to this orientation as "orientation III" in our previous work where we identified it as a distinct feature for the first time.[6,7] The existence of this orientation has been since confirmed by other researchers too at interfaces of alkylimidazolium NTf_2 ILs with vacuum and water.[8,19] As the opposite phase is replaced with cyclohexane, see Figure 7 b and e, the main features do not change qualitatively, however broadening of the peaks can be observed (i.e. they become noisier). In systems where the opposite phase is water (see Figure 7 c and f) a drastic qualitative change is observed in the orientation maps: "orientation III" becomes dominant while "orientation I" turns marginal and practically disappears from the map.

Trends in the orientational preferences of the butyl chains, displayed in Figure 8 a and b, are consistent with our observations made for the imidazolium rings. At both IL – vacuum interfaces the most probable orientation of butyl chains is to point towards the opposite phase along the surface normal ($\cos\sigma = 1$). In the case of BMIM NTf_2, a little secondary maximum appears too at $\cos\sigma = -1$ which means a little fraction of the butyl chains (undoubtedly belonging to imidazolium rings of orientation III) point inward, towards the bulk. The appearance of this peak can be explained with the less packed structure of the BMIM NTf_2 phase due to the larger size of the anion. When the opposite phase is cyclohexane slight quantitative but no qualitative changes can be observed: the distributions become less sharp (especially for BMIM NTf_2). At IL–water interfaces the picture changes qualitatively and the peak at $\cos\sigma = -1$ becomes dominant, though the distribution is very flat which renders all other orientations likely too. The orientational preferences of the $S \rightarrow C$ vectors (representing the "arms") of the NTf_2 anions show very similar changes upon variation of the opposite phase (see Figure 8 c). At the interfaces of BMIM NTf_2

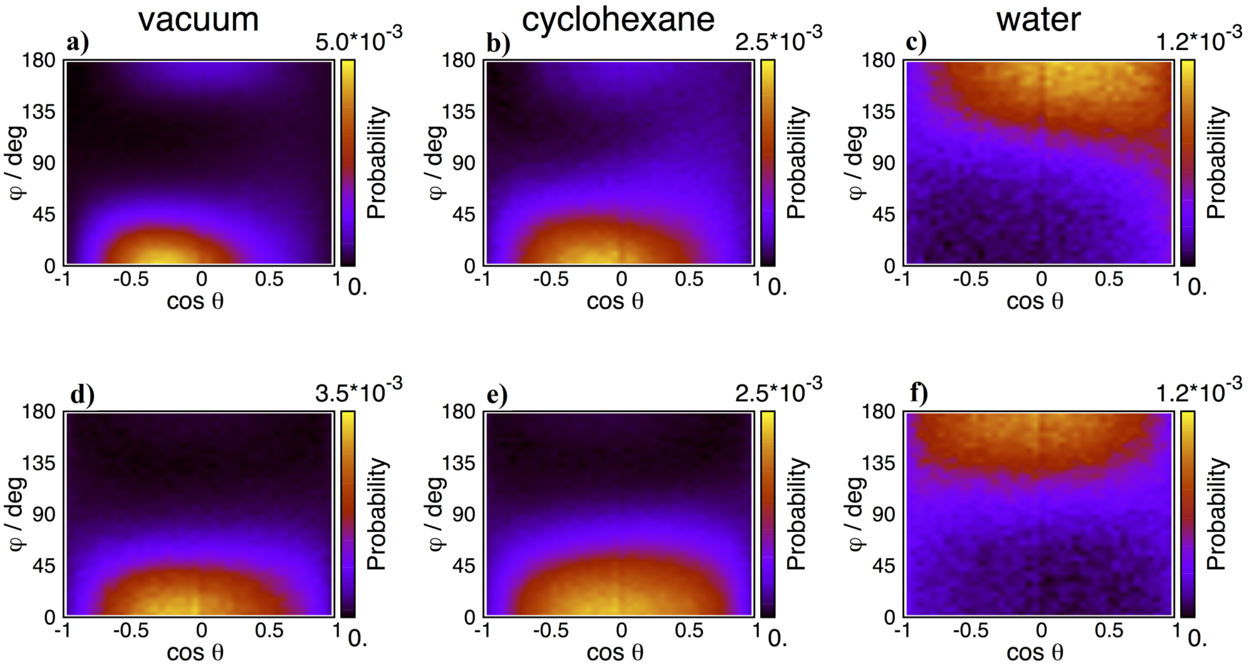

Figure 7: Preferred orientations of the imidazolium rings of the BMIM cations at the surface of the phases rich in BMIM NTf_2 (a-c) and BMIM PF_6 (d-f) when the opposite phases is either vacuum (a,d), cyclohexane (b,e) or water (c,f). The bivariate distributions are represented as 2D maps (for the definition of the coordinate frame see Figure 6). When water is the opposite phase cations turn with their butyl chains inside toward the bulk allowing polar ionic moieties become more exposed to the surface.

with vacuum and cyclohexane the most probable orientation of S→C vectors is an outward pointing direction along the surface normal. At the same time, a pronounced second peak can also be observed at $\cos\rho = -1$ which shows that a non-negligible fraction of the "arms" points inside, to the bulk. This conclusion is different from findings of former studies that concluded the NTf_2^- anions' both CF_3 groups point exclusively outwards to the vapor phases parallel with the surface normal.[8,11,18,19] We explain this by the rougher analysis performed in those studies that considered only the average orientation instead of a distribution of possible orientations. At the BMIM NTf_2 – water interface however this second peak becomes dominant implying that apolar "arms" have a high tendency to point inward. This change in the orientational preference of the anions was previously suggested by other simulation studies.[18,19] The picture emerging as a result of both the apolar butyl chains as well as the apolar “arms” of the anions pointing inward is again consistent with the increased appearance of polar groups observed in Section ’Distribution of surface atoms and molecules’. These changes imply among others a water-induced decrease in the hydrophobic character of the IL surface.

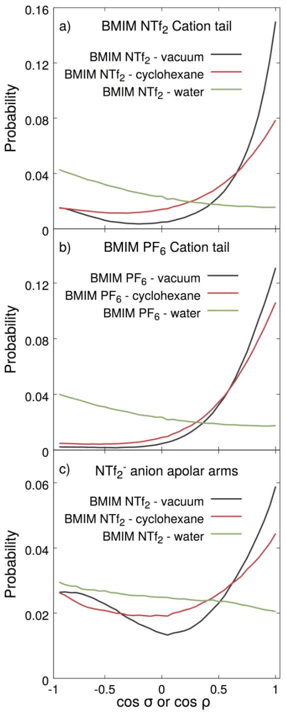

Figure 8: Distribution of orientation angles σ of butyl chains (described with the vector pointing from N1 to the last methyl group, C10, of the butyl chain, see Figure 1) of BMIM cations at surfaces involving BMIM NTf_2 (a) or BMIM PF_6 (b); and distribution of the angles ρ of the apolar arms of the NTf_2^- anions (represented by the vector pointing from the S atom to the C atom). For the definition of these angles see Figure 6. At interfaces with water, these apolar moieties tend to turn from the side of the opposite phase towards the IL bulk letting polar moieties become more exposed to the surface and hence promoting a less apolar overall character.

Molecular associations in the plane of the surface

In the last part of our analysis we investigated how molecular ordering changes in the plane of the surface. To this end, we computed two-dimensional radial distribution functions ($g^{2D}(r)$) in the (x,y) plane between certain moieties in the system. In particular, we were interested in how cations and anions associate with themselves or each other as well as how water associates with both the anion and the cation. We note that the surface, a 2D object by definition, is defined by atoms, however here we analyze entire surface molecules, hence we might sometimes consider pairs of atoms in our analysis whose projections on the (x,y) plane fall very close to each other though in reality one is effectively behind the other one (along the z direction). As a result, the 2D RDFs do not necessarily display zero at short distances. (Note that the increasing roughness leads to more of such situations thus increasing the shoulder at very short distances.)

In general, we observe the same trend for all kinds of 2D radial distribution functions: spatial correlations are strong and extend over the whole surface in IL – vacuum systems, but get somewhat dampened (meaning lowered peaks, but the a range of correlations does not change) as soon as the opposite phase is cyclohexane. The drastic change comes again when the opposite phase is water. As a result, for both ILs, the range of correlations becomes much shorter as well as peaks are flattened. We illustrate these trends with 2D radial distribution functions computed between surface anions and cations: Figure 9 shows the distribution function of radial distances between the central atoms of the anions and the center of mass of imidazolium rings (a and e), as well as between the three H atoms attached to the imidazolium rings and either the central P atom of PF_6^- anions (f-h) or the H-acceptor O atoms of the sulfonyl groups of NTf_2^- anions (b-d). 2D radial distribution functions computed between cation-cation and anion-anion pairs are shown in the Supporting information (Figure S1). Figure 9 illustrates well both the dampening of anion-cation correlations, and how the reported preference of both anions to associate with cations via the most acidic H atom of the ring (H2) vanishes at IL – water interfaces.

As water molecules can act both as H-donor and acceptor, in the last step we investigated if cation-anion associations are replaced with links between surface water molecules and cations or anions. Accordingly, we calculated 2D radial distribution functions between the O atoms of water molecules found at the surface of the IL rich phases and either the central

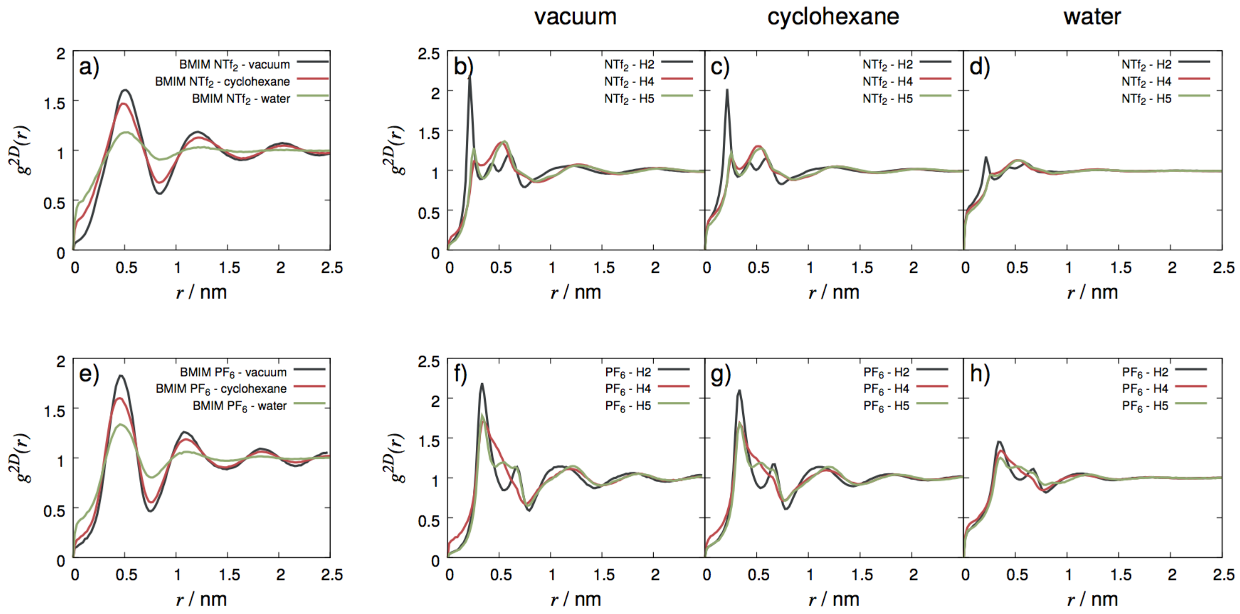

Figure 9: Anion-cation associations described by 2D radial distribution functions computed in the (x,y) plane (i.e. the plane of the macroscopic surface) between either the center of mass of the imidazolium ring and the central atom of anions (a,e) or between the three ring H atoms of the imidazolium ring and either the O atoms of NTf_2^- anions (b-d) or the P atom of PF_6^- anions (f-h). In the case of both IL species all cation-anion correlations get dampened as the opposite phase changes from vacuum through cyclohexane to water. The preference of the anion to bind with the most acidic H2 atom of the ring vanishes at the IL – water interfaces.

P or N atoms of surface anions (see Figure 10 a), or any of the three ring H atoms of the cation (see Figure 10 b, c). The displayed curves are somewhat noisy due to the relatively low occurrence of water molecules at the surface of the IL rich phases, but they clearly show that anions always associate with surface water molecules. On the contrary, cation–water associations are observed only in the BMIM NTf_2 – water system established uniquely through the most acidic H2 atom of the ring. We relate this simply to the higher ionic character of the $BMIM^+$ cation in combination with the NTf_2 anion. The importance of water–anion interactions over those between water molecules and cations has been reported by a series of quantum chemical as well as classical calculations performed both in gas phase and bulk.[43,54,55,77,78,80] Nonetheless, the possibility of forming weaker associations between cations and water was also evidenced experimentally and computationally through H atoms attached to the imidazolium ring, with a preference to interact with H2.[79,80]

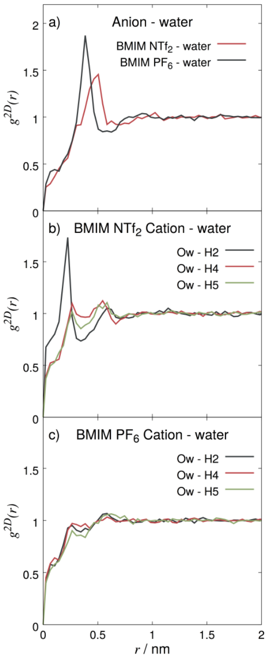

Figure 10: 2D radial distribution functions calculated in the (x,y) plane (i.e. the plane of the macroscopic surface) between the O atom of surface water molecules and either the central atom (N or P, respectively) of NTf_2^- and PF_6^- anions (a), or the 3 ring H atoms of BMIM cations at the surface of phases rich in either BMIM NTf_2 (b) or BMIM PF_2 (c). Water molecules do associate with both anions, however water-cation associations can be observed only in the case of BMIM NTf_2 through the most acidic H2 atom.

Summary and Conclusions

In this study we investigated, by means of molecular dynamics simulations, how the intrinsic structure of liquid/liquid interfaces involving ionic liquids changes upon varying the opposite fluid phase. Namely, we studied interfaces between ionic liquids and both an apolar liquid, cyclohexane, and a polar one, water. We chose to study two of the most popular ionic liquid species, both members of the alkylimidazolium family: 1-n-butyl-3-methylimidazolium hexafluorophosphate (BMIM PF_6) and 1-n-butyl-3-methylimidazolium bis(trifluoromethylsulfonyl)imid (BMIM NTf_2). As a reference, we also studied the corresponding IL – vacuum interfaces. Since the mutual miscibility in the studied biphasic systems is not negligible we applied a distance-based cluster search algorithm to unambiguously separate the fluid phases. The performance of the IL models was assessed through comparing computed interfacial tensions and equilibrium compositions to experimental values. We found the performance of the BMIM NTf_2 model acceptable, but we suspect that the model overrates the ionic character of the IL. Based on the same criteria, the performance of the BMIM PF_6 model was excellent. Furthermore, we found that solubility values estimated based on the size of the largest clusters determined with the cluster search algorithm agree reasonably well with those computed based on equilibrium densities, but the former approach tends to underestimate equilibrium compositions with increasing miscibilities. We explain this with the increasing theoretical ambiguity when it comes to separating highly mixed fluid phases and hence to defining the interface between them on the microscopic level.

In the next step we performed the ITIM analysis on the separated liquid phases in each sampled configuration and determined the list of surface atoms. We then carried out further analyses to assess, in particular, (i) both global and intrinsic ordering (by means of density profiles) along the surface normal, (ii) associations between surface ions and molecules in the plane of the surface, as well as (iii) the most preferred orientations of surface ions. Global density profiles, i.e. density correlations computed with respect to a flat surface, inevitably suffer from the smearing effect of thermally excited capillary waves compared to intrinsic density profiles that use the instantaneous atomic surface as a reference to compute density correlations. Accordingly, our global profiles showed much less structured shape compared to intrinsic profiles. We found that the structure of the surface of both ionic liquid rich phases gets disrupted (i.e. spatial correlations and orientational preferences are dampened) as soon as the opposite phase is either liquid instead of vacuum. Already the non-mixing apolar fluid weakens correlations, which are further reduced at IL – water interfaces. Furthermore, the surface of the phase rich in BMIM NTf_2 seemed to be affected more by water (i.e. the dampening of correlations was more pronounced) than the surface of the BMIM PF_6 rich phase, due probably to the higher solubility of water in BMIM NTf_2.

In contrast to what was observed at IL – vacuum interfaces, the tendency of surface anions to associate with surface cations is severely decreased and the preference of the anions to bind to cations through the most acidic ring hydrogen, H2, is almost totally wiped out at IL – water interfaces. While water molecules at the surface of both IL-rich phases tend to associate with anions, they associate with cations only in the case of the BMIM NTf_2 IL (through H2), which is rationalized by the stronger ionic character of the $BMIM^+$ cation in combination with the NTF_2^- anion. The surfaces of IL-rich phases are dominated by cations which, on the one hand, are bigger than either anion and, on the other hand, have a high tendency to point with their butyl chains toward vacuum (to a somewhat lesser extent also to cyclohexane) and thus cover anions. However, the surplus of cations at the surface almost vanishes at IL – water interfaces. Accordingly, we observed polar moieties being revealed and "pulled" to the surface from underlying intrinsic molecular layers. This was accompanied by a drastic change, irrespective of the anion, in the orientational preferences of cations as they turned with their butyl chains toward the bulk poiting with their methyl substituent to the water phase. Similarly, anions were found to have a higher tendency to turn with their apolar "arms" towards the bulk at BMIM NTf_2 – water interface. This increased appearance of polar moieties at IL – water interfaces shows a water-induced decrease of the apolar character and the adaptive capability of IL surfaces depending on the polarity of the opposite phase. In our subsequent study we plan to investigate the dynamics of transport through IL – water interfaces.

Acknowledgement

GH is thankful for financial support provided by COST Action MP 1305 ("Flowing Matter"). GH is an Eötvös postdoctoral fellow of the Hungarian Scholarship Board Office which is acknowledged. Financial support from ETN-COLLDENSE (H2020-MCSA-ITN-2014, Grant

No.642774) is also acknowledged. SK and GH thank the Austrian Research Fund (FWF): START-Projekt Y 627-N27.

Supporting Information

Snapshots of simulated systems that are not tractable by the proposed methodology (IL-hexanol and IL-benzene systems); interfacial tension and solubility data for IL – water systems calculated with 4 different water models; and various additional 2D radial distribution functions calculated at the surface of IL-rich phases are included.

References

(1) Welton, T. Room-Temperature Ionic Liquids. Solvents for Synthesis and Catalysis *Chem. Rev.* **1999**, *99*, 2071.

(2) Plechkova, N. V.; Seddon, K. R. Applications of Ionic Liquids in the Chemical Industry *Chem. Soc. Rev.* **2008**, *37*, 123-150.

(3) Castner, E. W. Jr.; Margulis, C. J.; Maroncelli, M.; Wishart J. F. Ionic Liquids: Structure and Photochemical Reactions *Annu. Rev. Phys. Chem.* **2011**, *62*, 85-105.

(4) Lovelock, K. R. J. Influence of the Ionic Liquid/Gas Surface on Ionic Liquid Chemistry *Phys. Chem. Chem. Phys.* **2012**, *14*, 5071-5089.

(5) Rowlinson, J. S.; Widom, B.; *Molecular Theory of Capillarity*; Clarendon press: Oxford, U.K., 1982.

(6) Hantal, G.; Cordeiro, M. N. D. S.; Jorge, M. What Does an Ionic Liquid Surface Really Look Like? Unprecedented Details from Molecular Simulations *Phys. Chem. Chem. Phys.* **2011**, *13*, 21230-21232.

(7) Hantal, G.; Voroshylova, I.; Cordeiro, M. N. D. S.; Jorge, M. A Systematic Molecular Simulation Study of Ionic Liquid Surfaces Using Intrinsic Analysis Methods *Phys. Chem. Chem. Phys.* **2012**, *14*, 5200-5213.

(8) Lísal, M.; Posel, Z.; Izák, P. AirLiquid Interfaces of Imidazolium-Based [TF_2N] Ionic Liquids: Insight from Molecular Dynamics Simulations *Phys. Chem. Chem. Phys.* **2012**, *14*, 5164-5177.

(9) Lísal, M.; Izák, P. Molecular Dynamics Simulations of n-Hexane at 1-Butyl-3-methylimidazolium Bis(trifluoromethylsulfonyl)imide Interface *J. Chem. Phys.* **2013**, *139*, 014704-1-15.

(10) Bhargava, B. L.; Balasubramanian S. Layering at an Ionic Liquid-Vapor Interface: A Molecular Dynamics Simulation Study of [Bmim][PF_6] *J. Am. Chem. Soc.* **2006**, *128*, 10073-10078.

(11) Perez-Blanco, M. E.; Maginn, E. Molecular Dynamics Simulations of CO2 at an Ionic Liquid Interface: Adsorption, Ordering, and Interfacial Crossing *J. Phys. Chem. B* **2010**, *114*, 11827-11837.

(12) Lynden-Bell, R. M. GasLiquid Interfaces of Room Temperature Ionic Liquids *Mol. Phys.* **2003**, *101*, 2625.

(13) Pensado, A. S.; Costa-Gomes, M. F.; Canongia-Lopes, J. N.; Malfreyt, P.; Pádua, A. A. H. Effect of Alkyl Chain Length and Hydroxyl Group Functionalization on the Surface Properties of Imidazolium Ionic Liquids *Phys. Chem. Chem. Phys.* **2011**, *13*, 13518-13526.

(14) Heggen, B.; Zhao, W.; Leroy, F.; Dammers, A. J.; Müller-Plathe, F. Interfacial Properties of an Ionic Liquid by Molecular Dynamics *J. Phys. Chem. B* **2010**, *114*, 6954-6961.

(15) Dang, L. X.; Wick, C. D. Anion Effects on Interfacial Absorption of Gases in Ionic Liquids. A Molecular Dynamics Study *J. Phys. Chem. B* **2011**, *115*, 6964-6970.

(16) Lynden-Bell, R. M.; Kohanoff, J.; del Pópolo, M. G. Simulation of Interfaces between Room Temperature Ionic Liquids and Other Liquids *Faraday Discuss.* **2005**, *129*, 57.

(17) Chaumont, A.; Schurhammer, R.; Wipff, G. Aqueous Interfaces with Hydrophobic Room-temperature Ionic Liquids: a Molecular Dynamics Study *J. Phys. Chem. B* **2005**, *109*, 18964-18973.

(18) Iwahashi, T.; Sakai, Y.; Kim, D.; Ishiyama, T.; Morita, A; Ouchi, Y. Nonlinear Vibrational Spectroscopic Studies on Water/Ionic Liquid([$C_n$mim]TFSA: n = 4, 8) Interfaces *Faraday Discuss.* **2012**, *154*, 289-301.

(19) Konieczny, J. K.; Szefczyk, B. Structure of Alkylimidazolium-Based Ionic Liquids at the Interface with Vacuum and Water – A Molecular Dynamics Study *J. Phys. Chem. B* **2015**, *119*, 3795-3807.

(20) Iwahashi, T.; Ishiyama, T.; Sakai, Y.; Morita, A; Kim, D.; Ouchi, Y. Liquid/Liquid Interface Layering of 1-butanol and [bmim]PF_6 Ionic Liquid: a Nonlinear Vibrational Spectroscopy and Molecular Dynamics Simulation Study *Phys. Chem. Chem. Phys.* **2015**, *17*, 24587.

(21) Linse, P. Monte Carlo Simulation of LiquidLiquid BenzeneWater Interface *J. Chem. Phys.* **1987**, *86*, 4177-4187.

(22) Benjamin, I. Theoretical Study of the Water/1, 2dichloroethane Interface: Structure, Dynamics, and Conformational Equilibria at the Liquidliquid Interface *J. Chem. Phys.* **1992**, *97*, 1432-1445.

(23) Chacón, E.; Tarazona, P. Intrinsic Profiles beyond the Capillary Wave Theory: a Monte Carlo Study *Phys. Rev. Lett.* **2003**, *91*, 166103.

(24) Chowdhary, J.; Ladanyi, B. M. Water-Hydrocarbon Interfaces: Effect of Hydrocarbon Branching on Interfacial Structure *J. Phys. Chem. B* **2006**, *110*, 15442-15453.

(25) Jorge, M.; Cordeiro, M. N. D. S. Intrinsic Structure and Dynamics of The Water/Nitrobenzene Interface *J. Phys. Chem. C* **2007**, *111*, 17612-17626.

(26) Pártay, L. B.; Hantal, G.; Jedlovszky, P.; Vincze, Á.; Horvai, G. A New Method for Determining the Interfacial Molecules and Characterizing the Surface Roughness in Computer Simulations. Application to the Liquid-Wapor Interface of Water *J. Comp. Chem.* **2008**, *29*, 945-956.

(27) Jorge, M.; Jedlovszky, P.; Cordeiro, M. N. D. S. A Critical Assessment of Methods for the Intrinsic Analysis of Liquid Interfaces. 1. Surface Site Distributions *J. Phys. Chem. C* **2010**, *114*, 11169-11179.

(28) Jorge, M.; Hantal, G.; Jedlovszky, P.; Cordeiro, M. N. D. S. A Critical Assessment of Methods for the Intrinsic Analysis of Liquid Interfaces. 2. Density profiles *J. Phys. Chem. C* **2010**, *114*, 18656-18663.

(29) Hantal, G.; Darvas, M.; Pártay, L. B.; Horvai, G.; Jedlovszky, P. Molecular Level Properties of the Water Surface at the Interface with Various Fluid Phases, as Seen from ITIM Analysis of Computer Simulation Results *J. Phys.: Condens. Matter* **2010**, *22*, 284112-1-14.

(30) Pártay, L. B.; Jedlovszky, P.; Horvai, G. Structure of the LiquidVapor Interface of WaterAcetonitrile Mixtures As Seen from Molecular Dynamics Simulations and Identification of Truly Interfacial Molecules Analysis *J. Phys. Chem. C* **2009**, *113*, 18173-18183.

(31) Pojják, K.; Darvas, M.; Horvai, G.; Jedlovszky, P. Properties of the LiquidVapor Interface of WaterDimethyl Sulfoxide Mixtures. A Molecular Dynamics Simulation and ITIM Analysis Study *J. Phys. Chem. C* **2010**, *114*, 12207-12220.

(32) Pártay, L. B.; Horvai, G.; Jedlovszky, P. Temperature and Pressure Dependence of the Properties of the LiquidLiquid Interface. A Computer Simulation and Identification of the Truly Interfacial Molecules Investigation of the WaterBenzene System *J. Phys. Chem. C* **2010**, *114*, 21681-21693.

(33) Hantal, G.; Terleczky, P.; Horvai, G.; Nyulaászi, L.; Jedlovszky, P. Molecular Level Properties of the Water-Dichloromethane Liquid/Liquid Interface, as Seen from Molecular Dynamics Simulation and Identification of Truly Interfacial Molecules Analysis. *J. Phys. Chem. C* **2009**, *113*, 19263-19276.

(34) Darvas, M.; Pártay, L. B.; Jedlovszky, P.; Horvai, G. Temperature Dependence of the Lateral Hydrogen Bonded Clusters of Molecules at the Free Water Surface *J. Mol. Liq.* **2012**, *153*, 88-93.

(35) Abrankó-Rideg, N.; Darvas, M.; Horvai, G.; Jedlovszky, P. Immersion Depth of Surfactants at the Free Water Surface: A Computer Simulation and ITIM Analysis Study *J. Phys. Chem. B* **2013**, *117*, 8733-8746.

(36) Fábián, B.; Szőri, M.; Jedlovszky, P. Floating Patches of HCN at the Surface of Their Aqueous Solutions Can They Make HCN World Plausible? *J. Phys. Chem. C* **2014**, *118*, 21469-21482.

(37) Hess, B.; Kutzner, C.; van der Spoel, D.; Lindahl, E. GROMACS 4: Algorithms for Highly Efficient, Load-Balanced, and Scalable Molecular Simulation *J. Chem. Theory Comp.* **2008**, *4*, 435-447.

(38) Visser, A. E.; Swatloski, R. P.; Reichert, W. M.; Griffin, R. T.; Rogers. R. D. Traditional Extractants in Nontraditional Solvents: Groups 1 and 2 Extraction by Crown Ethers in Room-Temperature Ionic Liquids *Ind. Eng. Chem. Res.* **2000**, *39*, 3596-3604.

(39) Niedermeyer, H.; Hallett, J. P.; Villar-Garcia, I. P.; Hunt, P. A.; Welton, T. Mixtures of Ionic Liquids *Chem. Soc. Rev.* **2012**, *41*, 7780-7802.

(40) Jiang, W.; Wang, Y.; Voth, G. A. Molecular Dynamics Simulation of Nanostructural Organization in Ionic Liquid/Water Mixtures *J. Phys. Chem. B* **2007**, *111*, 4812-4818.

(41) Bhargava, B. L.; Yasaka, Y.; Klein, M. L. Computational Studies of Room Temperature Ionic LiquidWater Mixtures *Chem. Comm.* **2011**, *47*, 6228-6241.

(42) Hanke, C. G.; Lynden-Bell, R. M. A Simulation Study of Water-Dialkylimidazolium Ionic Liquid Mixtures *J. Phys. Chem. B* **2003**, *107*, 10873-10878.

(43) Danten, Y.; Cabaço, M. I.; Besnard, M. Interaction of Water Highly Diluted in 1-Alkyl-3-methyl Imidazolium Ionic Liquids with the PF_6 and BF_4 Anions *J. Phys. Chem. A* **2009**, *113*, 2873-2889.

(44) Kohno, Y.; Ohno, H. Ionic Liquid/Water Mixtures: From Hostility to Conciliation *Chem. Comm.* **2012**, *48*, 7119-7130.

(45) van der Spoel, D.; Lindahl, E.; Hess, B.; Groenhof, G.; Mark, A. E.; Berendsen, H. J. C. GROMACS: Fast, Flexible, and Free *J. Comp. Chem.* **2005**, *26*, 1701-1718.

(46) Nosé, S. A Molecular Dynamics Method for Simulations in the Canonical Ensemble *Mol. Phys.* **1984**, *52*, 255.

(47) Hoover, W. Canonical Dynamics: Equilibrium Phase-space Distributions *Phys. Rev. A* **1985**, *31*, 1695.

(48) Parrinello, M.; Rahman, A. Polymorphic Transitions in Single Crystals: A New Molecular Dynamics Method *J. Appl. Phys.* **1981**, *52*, 7182.

(49) Essmann, U.; Perera, L.; Berkowitz, M. L.; Darden, T.; Lee, H.; Pedersen, L. G. A Smooth particle Mesh Ewald Method *J. Chem. Phys.* **1995**, *103*, 8577-8592.

(50) Smith, E. R. Electrostatic Energy in Ionic Crystals *Proc. R. Soc. London, Ser. A* **1981**, *375*, 475.

(51) Yeh, I.-C.; Berkowitz M. L. Ewald Summation for Systems with Slab Geometry *J. Chem. Phys.* **1999**, *111*, 3155-3162.

(52) Arnold, A.; de Joannis, J.; Holm, C. Electrostatics in Periodic Slab Geometries. I *J. Chem. Phys.* **2002**, *117*, 2496-2502.

(53) Bhargava, B. L.; Balasubramanian S. Refined Potential Model for Atomistic Simulations of Ionic Liquid [bmim][PF_6] *J. Chem. Phys.* **2007**, *127*, 114510.

(54) Dommert, F.; Wendler, K.; Qiao, B.; Delle Site, L.; Holm, C. Generic Force Fields for Ionic Liquids *J. Mol. Liq.* **2014**, *192*, 32-37.

(55) Izgorodina, E. I.; Forsyth, M.; MacFarlane, D. R. Towards a Better Understanding of 'Delocalized Charge' in Ionic Liquid Anions *Aus. J. Chem.* **2008**, *60*, 15-20.

(56) Youngs, T. G. A., Hardacre, C. Application of Static Charge Transfer Within an IonicLiquid Force Field and its Effect on Structure and Dynamics *Chem. Phys. Chem.* **2008**, *9*, 1548.

(57) Koeddermann, T.; Paschek, D.; Ludwig, R. Molecular Dynamic Simulations of Ionic Liquids: A Reliable Description of Structure, Thermodynamics and Dynamics *Chem. Phys. Chem.* **2007**, *8*, 2464-2470.

(58) Canongia-Lopes, J. N.; Deschamps, J.; Pádua, A. A. H. Modeling Ionic Liquids Using a Systematic All-Atom Force Field *J. Phys. Chem. B* **2004**, *108*, 2038.

(59) Jorgensen, W. L.; Chandrasekhar, J.; Madura, J. D.; Impey, R. W.; Klein, M. L. Comparison of Simple Potential Functions for Simulating Liquid Water *J. Chem. Phys.* **1983**, *79*, 926-935.

(60) Logotheti, G.-E.; Ramos, J.; Economou I. G. Molecular Modeling of Imidazolium-based [Tf_2N] Ionic Liquids: Microscopic Structure, Thermodynamic and Dynamic Properties, and Segmental Dynamics *J. Phys. Chem. B* **2009**, *113*, 7211-7224.

(61) Blanchard, L. A.; Brennecke, J. F. Recovery of Organic Products from Ionic Liquids Using Supercritical Carbon Dioxide *Ind. Eng. Chem. Res.* **2001**, *40*, 287-292.

(62) Berendsen, H. J. C.; Postma, J. P. M.; van Gunsteren, W. F.; and Hermans, J. In *Intermolecular Forces*, p. 331, edited by B. Pullman, Reidel: Dordrecht, 1981.

(63) Sega, M.; Kantorovich, S.; Jedlovszky, P.; Jorge, M. The Generalized Identification of Truly Interfacial Molecules (ITIM) Algorithm for Nonplanar Interfaces *J. Chem. Phys.* **2013**, *138*, 044110-1-10.

(64) Allen, M. P.; Tildesley, D. J. *Computer Simulation of Liquids*, Oxford University Press: Bristol, UK, 1989.

(65) Rogers, R. D.; Seddon, K. R.; Volkov, S. ed. *Green Industrial Applications of Ionic Liquids*, Springer: Dordrecht, The Netherlands, 2002.

(66) Freire, M. G.; Carvalho, P. J.; Gardas, R. L.; Marrucho, I. M.; Santos, L. M. N. B. F.; Coutinho, J. A. P. Mutual Solubilities of Water and the [$C_n$mim][Tf_2N] Hydrophobic Ionic Liquids *J. Phys. Chem. B*, **2008**, *112*, 1604-1610.

(67) Freire, M. G.; Neves, C. M. S. S.; Ventura, S. P. M.; Pratas, M. J.; Marrucho, I. M.; Oliveira, J.; Coutinho, J. A. P.; Fernandes, A. M. Solubility of Non-aromatic Ionic Liquids in Water and Correlation Using a QSPR Approach *Fluid Phase Equilib.* **2010**, *294*, 234-240.

(68) Li, Y.; Wang, L.-S.; Cai, S.-F. Mutual Solubility of Alkyl Imidazolium Hexafluorophosphate Ionic Liquids and Water *J. Chem. Eng. Data* **2010**, *55*, 5289-5293.

(69) Klomfar, J.; Souckova, M.; Patek, J. Surface Tension Measurements with Validated Accuracy for Four 1-alkyl-3-methylimidazolium Based Ionic Liquids *J. Chem. Thermodyn.* **2010**, *42*, 323-329.

(70) Carrera, G. V. S. M.; Afonso, C. A. M.; Branco, L. C. Interfacial Properties, Densities, and Contact Angles of Task Specific Ionic Liquids *J. Chem. Eng. Data* **2010**, em 55, 609-615.

(71) Gardas, R. L.; Ge, R.; Manan, N. A.; Rooney, D. W.; Hardacre, C. Interfacial Tensions of Imidazolium-based Ionic Liquids with Water and n-alkanes *Fluid Phase Equilib.* **2010**, *294*, 139-147.

(72) Almeida, H. F. D.; Teles, A. R. R.; Lopes-da-Silva, J. A.; Coutinho, J. A. P.; Freire, M. G. Influence of the Anion on the Surface Tension of 1-ethyl-3-methylimidazolium-based Ionic Liquids *J. Chem. Thermodyn.* **2012**, *54*, 49-54.

(73) Kilaru, P.; Baker, G. A.; Scovazzo, P. Density and Surface Tension Measurements of Imidazolium-, Quaternary Phosphonium-, and Ammonium-based Room-temperature Ionic Liquids: Data and Correlations *J. Chem. Eng. Data* **2007**, *52*, 2306-2314.

(74) Jiqin, Z.; Jian, C.; Chengyue, L.; Weiyang, F. Viscosities and Interfacial Properties of 1-methyl-3-butylimidazolium Hexafluorophosphate and 1-isobutenyl-3-methylimidazolium Tetrafluoroborate Ionic Liquids *J. Chem. Eng. Data* **2007**, *52*, 812-816.

(75) Dominguez, I.; Gonzalez, E. J.; Palomar, J.; Dominguez, A. Phase Behavior of Ternary Mixtures Aliphatic Hydrocarbon + Aromatic Hydrocarbon + Ionic Liquid: Experimental LLE Data and Their Modeling by COSMO-RS *J. Chem. Thermodyn.* **2014**, *77*, 222-229.

(76) Jedlovszky, P.; Vincze, Á.; Horvai, G. New insight into the Orientational Order of

Water Molecules at the Water/1,2-dichloroethane Interface: a Monte Carlo Simulation Study *J. Chem. Phys.* **2002**, *117*, 2271.

(77) Schröder, C.; Rudas, T.; Neumayr, G.; Benkner, S.; Steinhauser, O. On the Collective Network of Ionic Liquid/Water Mixtures. I. Orientational Structure *J. Chem. Phys.* **2007**, *127*, 234503.

(78) Rezabal, E.; Schäfer, T. First Principle Approach to Solvation by Methylimidazolium-based Ionic Liquids *J. Phys. Chem. B* **2013**, *117*, 553-562.

(79) Chang, H.-C.; Jiang, J.-Ch.; Chang, Ch.-Y.; Su, J.-Ch.; Hung, Ch.-H.; Liou, Y.-Ch.; Lin, S. H. Structural Organization in Aqueous Solutions of 1-Butyl-3-methylimidazolium Halides: A High-Pressure Infrared Spectroscopic Study on Ionic Liquids *J. Phys. Chem. B* **2008**, *112*, 4351-4356.

(80) Rezabal, E.; Schäfer, T. Ionic Liquids as Solvents of Polar and Non-polar Solutes: Affinity and Coordination *Phys. Chem. Chem. Phys.* **2015**, *17*, 14588-14597.

Graphical TOC Entry